Al-Nahrain Journal of Science
ANJS, Vol. 28 (1), March, 2025, pp. 132 – 142

The Relationship between Exposure to Radon in Majnoon Field and Lung Cancer Risk

Ali Khalid Sheihab[1], Sohaib Qusay[2,*], Asia H. Al-Mashhadani[1]

[1]Department of Physics, College of Science, Baghdad University, Jadiriya, Baghdad, Iraq
[2]Department of Physics, College of Science, Al-Nahrain University, Jadiriya, Baghdad, Iraq

Article's Information

Received: 13.04.2024
Accepted: 10.11.2024
Published: 15.03.2025

Keywords:
Majnoon oil field
deaths per million people
Rn concentrations

Abstract

A comprehensive assessment of lung cancer risk resulting from radon gas exposure originating from the Majnoon oil fields in Basra in 2021 was conducted. Previous studies indicate a notable surge in the incidence of lung cancer in 1991, with reported cases reaching 5720. In 2019, this number escalated significantly to 35864, underscoring a substantial increase in the number of cases over the years. A detailed evaluation of lung cancer risk associated with both indoor and outdoor exposure to naturally occurring ^{222}Rn gas was performed. The study employed CR-39 detectors to measure radon concentrations both within and surrounding the oil field. Notably, the highest concentration was detected in the sample taken at a depth of 1350 m and was 11.80 Bq/m^3, while the lowest concentration was observed in a sample taken at a depth of 1450 m was 2.18 Bq/m^3. The calculated average cancer risk attributable to radon exposure was determined to be 4 deaths per million people. This underscores the potential health impact of radon gas in the Majnoon oil fields and emphasizes the need for further studies and interventions to mitigate the associated risks.

http://doi.org/10.22401/ANJS.28.1.15
*Corresponding author: suhaib.qusay@nahrainuniv.edu.iq

1. Introduction

Cancer stands as a prominent contributor to morbidity and mortality in Iraq, ranking as the second leading cause of death at 9.6%, following cardiovascular diseases. The assessment of cancer risk typically relies on epidemiological studies that analyze the occurrence of specific disorders within distinct population cohorts. To gauge the elevated incidence of cancer, it is imperative to quantify the number of individuals exposed to radiation along with the corresponding doses administered. A methodological approach involves contrasting these figures with those from non-irradiated groups, enabling the observation of the anticipated cancer rates. This analytical process entails a comprehensive exploration of the biological effects induced by low levels of ionizing radiation. Through this examination, a clearer understanding of the correlation between radiation exposure and cancer occurrence can be elucidated offering valuable insights for informed public health strategies [1]. In recent years, there has been a heightened comprehension of physiological factors that modulate health outcomes, notably gender and age. While the overall risk of tumor induction due to sex-related factors is relatively low, it exhibits variability across different anatomical sites. Specifically, the absolute risk of developing most solid cancers tends to be higher in women compared to men. Moreover, age is recognized as a crucial determinant, with young individuals facing both higher relative and absolute risks than their older counterparts when subjected to radiation. It is important to note that these risks can vary based on the specific location under consideration. Tables 1 and 2, along with Fig. 1, outline population risk factors for fatal cancers across different organs, as established by the International Commission on Radiological Protection (ICRP) [2]. This data provides a comprehensive reference for understanding the nuanced dynamics of cancer risks associated with gender, age, and specific anatomical sites. Risk factors exhibit variations among different populations due to distinct age distributions within these groups. For example, the risk factor differs

between the general population and the labor force, considering that the average age of the labor force tends to be higher than that of the general population [3]. Consequently, the risk factor for the labor force is generally lower when compared to the risk factor for the general population. The primary objective of this continuous study is to assess the risk of developing lung cancer linked to exposure to naturally occurring ^{222}Rn gas, both indoors and outdoors. This evaluation involves the utilization of CR-39 detectors to measure Rn concentrations within and outside the boundaries of the oil field. By employing this method, the study aims to gain insights into the potential health risks posed by radon exposure in both indoor and outdoor environments, with a specific focus on the oil field under consideration.

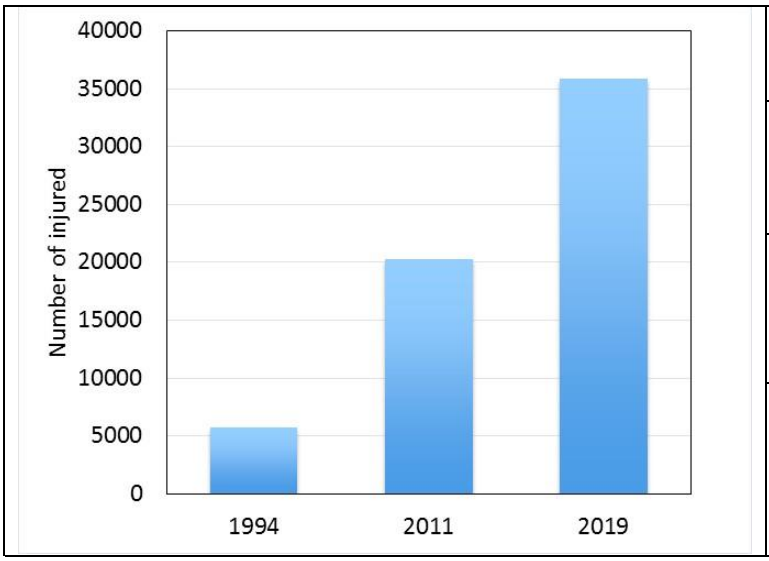

Number of injured	Population	Year
5720	19540613	1994
20278	30735365	2011
35864	39127889	2019

Figure 1. Numbers of casualties compared to the population in Iraq, Number of Cancer cases [3]

Table 1. Population of the people with cancer in Al-Basreh Governorate by gender 2006 [4].

Gender	Males No.	%	Female No.	%	Total No	%
Al-Basreh	943442	6.51	930200	6.50	1873642	13.01

Table 2. Distribution of the top ten cancers in Al-Basra, Iraq, 2019 [4].

	Top Ten Total	No.	%
1	Breast	467	19
2	Bronchus & Lung	160	6.59
3	Leukemia	150	6.18
4	Colorectal	145	5.97
5	Brain & Other CNS	140	5.77
6	Non-Hodgkin Lymphoma	139	5.72
7	Urinary Bladder	132	5.44
8	Stomach	80	3.29
9	Kidney	77	3.17
10	Thyroid Gland	74	3.05
11	Total Top Ten	1564	64.42
12	Total other Site	864	35.58
	Total	2428	100%

1.1. Excess lifetime cancer risk (ELCR) for soil

The excess lifetime cancer risk denotes the likelihood of developing cancer over an individual's lifetime at a specific exposure level. This metric is expressed as a numerical value, representing the additional cases of cancer anticipated within a particular population

when exposed to a carcinogenic substance at a specified dose. ELCR is computed using Equation 1, taking into account an average human lifespan of 70 years. This calculation provides a quantitative measure of the supplementary cancer risk associated with a particular level of exposure to the carcinogen [5].

$$ELCR = AEDE \times DL \times RF \quad \dots (1)$$

In the provided equation, AEDE (Annual Effective Dose Equivalent) signifies the yearly measure of the effective radiation dose. DL denotes the average Duration of Life, which is assumed to be 70 years, while RF represents the risk factor, expressed in Sv^{-1} (Sieverts per inverse year), indicating the probability of fatal cancer risk per Sievert. This is particularly relevant for low dose background radiations associated with stochastic effects, the International Commission on Radiological Protection (ICRP) 60 prescribes a value of 0.05 for public exposure [6, 7]. This value is dimensionless, representing the likelihood of cancer incidence. Substituting this value into the equation allows us to derive the relationship mentioned above.

1.2. Concentration of Radon

The evaluation of radon exposure and its decay products requires a thorough consideration of the actual activity concentrations of various alpha-emitting radionuclide series present in the inhaled air. This is critical due to the substantial influence of the total alpha particle energy released during or following the decay of these inhaled radionuclides on the resultant radiation dose. Therefore, the conceptual definition of radon exposure rate is expressed in terms of potential alpha energy concentration (PAEC), measured in joules per cubic meter ($J\ m^{-3}$) or as working level (WL) [8]. This definition is based on the assumption that one liter of air contains 100 pCi (3.7 Bq) of 222Rn, with each of its four short-lived progeny in secular equilibrium with it, meaning each daughter has an activity of 3.7 Bq. The EPA recommends remediation of homes if radon levels reach 4 pCi/L (picocuries per liter) or higher. Given that no safe level of radon exposure has been established, the EPA also advises Americans to consider remediation for radon levels between 2 pCi/L and 4 pCi/L. The average indoor radon concentration in American homes is approximately 1.3 pCi/L. According to the Environmental Protection Agency (EPA), this national average leads to an estimated 21,000 lung cancer cases annually attributable to radon exposure. In comparison, the average radon concentration in outdoor air is about 0.4 pCi/L, which is one-tenth of the EPA's recommended action level of 4 pCi/L.[9].

2. Methods for Calculating Attributable Risk for Radon

2.1. Sample preparation of soil

A total of sixty soil samples were systematically gathered from wells located within the Majnoon oil field (MJ-95) in Basra city, Iraq, in 2021 as illustrated in Figure 2. This focused study was conducted exclusively in the Basrah Governorate, home to the Majnoon oil field. Notably, the Basra region holds significance in hydrogeological perspectives due to its abundance of oil fields and underlying groundwater reservoirs. The geographical concentration of these resources makes the Basra region noteworthy for hydrogeological investigations. Soil samples were extracted from various depths within the MJ-95 well, and subsequently, the collected soil underwent a blending process and was crushed to achieve a particle size small enough to pass through a 0.2 mm electric mesh sieve. The entirety of the samples, having undergone this preparation, was then carefully weighed using a high-sensitivity digital scale with an accuracy of ± 0.01%, and each sample was standardized to a weight of 50 grams.

2.2. Solid State Nuclear Track Detectors SSNTDs

The domain of solid-state nuclear track detectors (SSNTDs) has witnessed significant and comprehensive advancements, leading to their widespread application across diverse fields of science and technology. The unique track-recording properties of insulating solids were initially unveiled at the Atomic Energy Research Establishment (AERE) [10]. The tracks of alpha particles are directly observed using an electron microscope following selective chemical etching with an optical microscope for further examination.

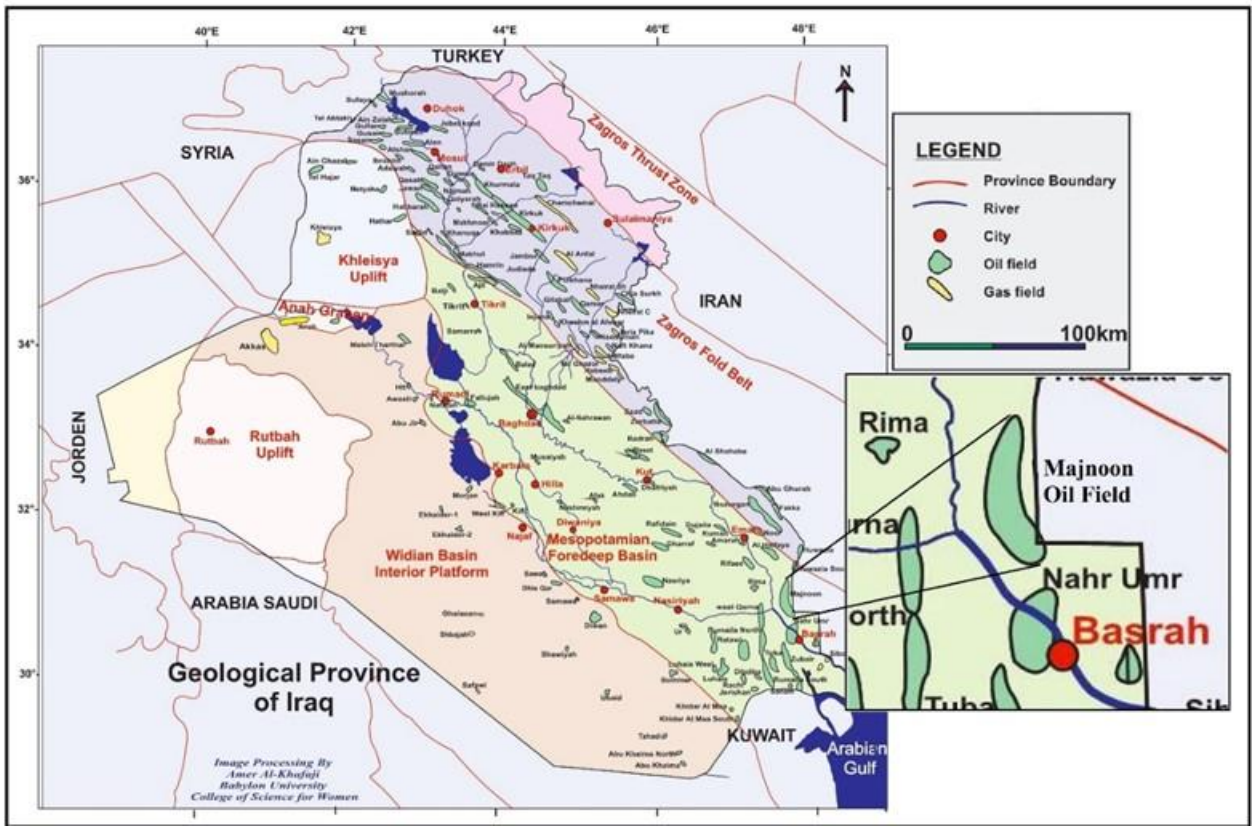

Figure 2. Majnoon oil field in Basra, south of Iraq [11].

Soil samples were extracted from various depths within the MJ-95 well, and subsequently, the collected soil underwent a blending process and was crushed to achieve a particle size small enough to pass through a 0.2 mm electric mesh sieve. The entirety of the samples, having undergone this preparation, was then carefully weighed using a high-sensitivity digital scale with an accuracy of ± 0.01%, and each sample was standardized to a weight of 50 grams.

2.3. Solid State Nuclear Track Detectors SSNTDs

The domain of solid-state nuclear track detectors (SSNTDs) has witnessed significant and comprehensive advancements, leading to their widespread application across diverse fields of science and technology. The unique track-recording properties of insulating solids were initially unveiled at the Atomic Energy Research Establishment (AERE) [9, 10]. The tracks of alpha particles are directly observed using an electron microscope following selective chemical etching with an optical microscope for further examination.

2.4. Track geometry

Various parameters were employed to characterize the geometry of etched tracks, including:

1. The full length of the latent track (L).
2. The thickness of the surface removed by etching (h).
3. The diameter of the etch pit (D). The track length (L) at etching time (t) given by the following relation:

$$L = V_T . t \qquad ...(2)$$

The surface (R) is also beginning removed at a rate V_B, so that:

$$R = V_T . t - V_B . t \qquad ...(3)$$

where: V_T is the track etch rate, V_B is bulk etch rate. When the track etch rate (V_T) is constant and the particle penetrates normally, then the surface thickness (h) is given by

$$h = V_B . t \qquad ...(4)$$

The diameter of etch pit (D) is related to V_B and V_T according to the following equation:

$$D = 2V_B . \left[\frac{V_T - V_B)}{V_T + V_B)}\right] \qquad ... (5)$$

Equation 5 illustrates that the diameter of the track (D) and the length of the etched track (L) are predominantly affected by the competing effects of the track etch rate (VT) and the bulk etch rate (VB). When VT is equal to VB, both the length (L) and diameter (D) of the track become zero, resulting in the absence of track formation. [12].

2.5. The chemical form of CR-39

The commercially available allyl diglycol carbonate detector, widely referred to as CR-39, is produced through the polymerization of oxydi-2,1-ethanediyl di-2-propenyl ester of carbonic acid. This process utilizes an allyl resin monomer, characterized by the presence of the following functional group. [13]. [CH_2 =CH=CH_2] The monomer, depicted in Figure 3, inherently possesses two of these functional groups. The CR-39 detector, derived from this monomer, exhibits notable efficiency in recording particle tracks when compared to other detectors. Its distinctive features include optical transparency, high sensitivity to radiation, excellent isotropy, and homogeneity. Additionally, CR-39 does not undergo cross-linking following radiation-induced disruption of chemical bonds. It is compatible with non-solvent chemical etchants and exhibits resistance to a broad spectrum of solvents, maintaining its integrity against the effects of heating.

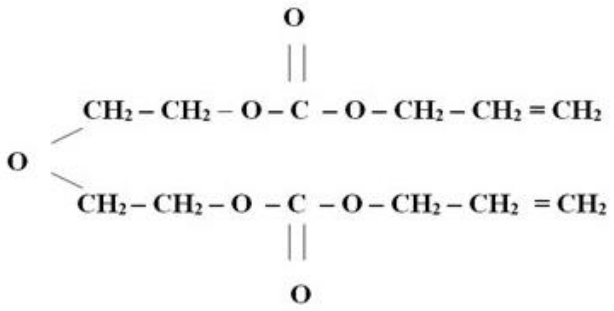

Figure 3. The chemical form of CR-39 plastic.

Beyond a threshold of approximately 7.9 MeV, the inelastic breakup of 12C into alpha particles becomes feasible, and the energy lost by the neutron is distributed among the three alpha particles. Upon undergoing chemical etching with a caustic solution, the CR-39 polymer experiences selective removal of fragments from disrupted bonds. This chemical modification leads to the formation of a pit within the material [14].

2.6. The chemical etching

When ionizing particles traverse polymeric track detectors, they generate latent tracks, which are essentially imprints of radiation-induced damage. [15]. The most effective method for observing these tracks involves etching the solid-state nuclear track detector (SSNTD) material with a chemical solution. This solution specifically acts on the impaired material, enlarging the initial track to a dimension that is discernible when examined under an optical microscope. This process elucidates the fundamental features of the nuclear track etch technique [16]. This technique functions as a single-particle drilling tool, offering adjustability in hole diameter, uniformity in hole size, length, and orientation, as well as flexibility in hole density. Notably, it is applicable to a diverse range of materials. The etching procedure entails the swift dissolution of the disordered section within the core of the track, which is distinguished by a higher free energy state compared to the intact bulk material [17]. The selected reagent must demonstrate the ability to delicately etch the bulk material while specifically focusing on the paths of particle-induced damage. As depicted in Figure 4, the track etching process is illustrated [18]. The trails of radiation damage generated by charged particles comprise a disordered structure associated with an elevated free energy state, indicating areas of heightened chemical activity. These areas selectively dissolve, and their dimensions expand upon exposure to an etching solution.

2.7. The etchant solution

Sodium hydroxide solution with 6.25N normality has been used for the etching process, prepared as:

$$W = Weq \times N \times V \qquad (6)$$

where:
W = the weight of NaOH needed to prepare the given normality.
W_{eq} =equivalent weight of NaOH = 40.
N = normality = 6.25.
V = volume of distilled water=250 ml.
The etchant compartment, with an approximate volume of 250 ml, is engineered as a sealed assembly. It is equipped with a small vent located at the top of the condenser tube to prevent alterations in the etchant's normality (concentration) due to evaporation during the experiment. The etching process was conducted at a constant temperature of 70°C, with a total duration of 7 hours.

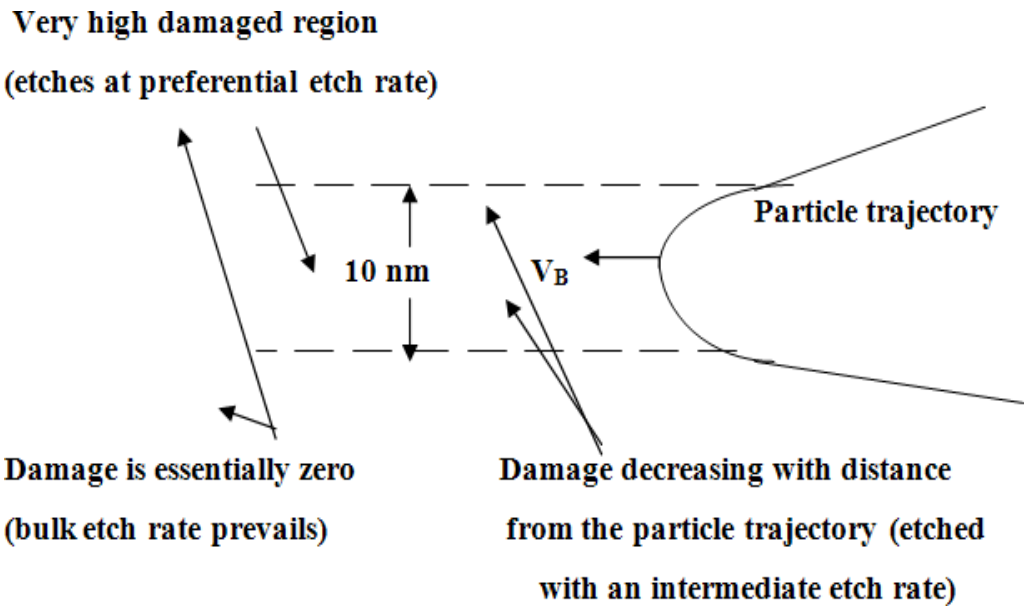

Figure 4. Track etching process [16]

2.8. Measurement the Radon Concentration in Soil

The significant risks posed to human health by exposure to radon and its progeny have spurred numerous studies aiming to determine radon concentrations in various environments, including residential homes. The presence of radon and its daughter products within houses can be attributed to diverse sources, such as building materials and the soil beneath the houses. In this study, the radon cup technique was employed, utilizing a cylindrical chamber measuring 4 cm in diameter and 10 cm in height. This chamber was placed inside the detector, impacting the solid-state nuclear track detector CR-39 (refer to Fig. 5). These detectors underwent an etching process using 6.25 N sodium hydroxide at a temperature of 70°C for a duration of 7 hours. Subsequently, the tracks were meticulously counted using a "NOVEL" type optical microscope. The track density was determined by averaging the total number of tracks and dividing by the area of the field of view. CR-39 detectors are employed for prolonged assessments of radon exhalation rates. Plastic track detectors, functioning as passive devices, are utilized for radon measurements both within homes and in field settings. It is essential to recognize that ^{222}Rn and its short-lived decay products are significant contributors to the effective dose received by the population due to natural radiation. [18]. The formula used to measure track density of detector CR-39 was as follows:

$$Track\ Density\ (\rho)\ (\frac{Track}{Cm^2}) = \frac{Average\ of\ Total\ Track}{Area\ of\ Feild\ of\ View} \quad \ldots(7)$$

Figure 5. Radon cup technique.

2.9. Calculation of radon concentration (CRn)

Following this duration, the detectors were gathered and subjected to chemical etching using 6N sodium hydroxide (NaOH) at 70°C for 7 hours. Subsequently, the tracks of alpha damage were enumerated using an optical microscope with a magnification of 400X. Radon concentration (C_{Rn}) was calculated by:

$$C_{Rn}\left(\frac{Bq}{m^3}\right) = \frac{C_0 t_0 p}{p_0 t} \quad \ldots(8)$$

In the given equation, Co stands for the activity concentration of a standard source, to represents the exposure time for the standard source, p_0 is the track density for the standard source (measured in tracks per square centimeter), p denotes the track density for the detector (also in tracks per square centimeter), and t indicates the exposure time of the detector.

3. Results and Discussion

Table 3 shows the majority of estimating the Excess lifetime cancer risk for exposure to ^{222}Rn in Majanoon field which are ranged from 2.185445 at 1450 m to 11.80140 at 1350 m with average value 4.76, this value falls within the high risk levels, i.e there are 4.76 deaths per million for indoor and outdoor exposures of ^{222}Rn, respectively. The radium concentrations ranged between (428.75 – 79.36) Becquerel / m^3, and the highest recommended limit UNSCEAR (50-150) Bq / m^3 [19, 20]. The findings underscore the imperative need to address radon exposure and its associated health risks to safeguard public health and mitigate cancer incidence. It is particularly crucial to prioritize the estimation of the number of lung cancer cases potentially induced by ^{222}Rn in regions where oil field operations are conducted. Further epidemiological studies need to be conducted to test the proposed hypothesis.

Table 3. C_{Rn} & H_e and ELCR in soil sample contained natural radionuclide.

Sample	Depth m	C_{Rn} (Bq/m^3)	H_e (msv/y)	ELCR
S1	190	142.86	1.0218	3.934
S2	790	126.98	0.9082	3.497
S3	900	95.238	0.6812	2.623
S4	950	111.11	0.7947	3.0596
S5	1000	222.22	1.5894	6.119
S6	1050	126.98	0.9082	3.496
S7	1070	190.48	1.3624	5.245
S8	1100	158.73	1.1353	4.371
S9	1125	111.11	0.7947	3.0596
S10	1150	111.11	0.7947	3.0596
S11	1200	142.86	1.0218	3.934
S12	1230	142.86	1.0218	3.934
S13	1250	158.73	1.1353	4.371
S14	1290	111.11	0.7947	3.0596
S15	1300	142.86	1.0218	3.934
S16	1350	428.57	3.0653	11.801
S17	1400	174.6	1.2488	4.808
S18	1450	79.365	0.5676	2.185
S19	1475	238.1	1.7029	6.556
S20	1500	95.238	0.6812	2.623
S21	1550	142.86	1.0218	3.934
S22	1600	126.98	0.9082	3.498
S23	1650	111.11	0.7947	3.0596
S24	1700	190.48	1.3624	5.245
S25	1730	174.6	1.2488	4.808
S26	1750	349.21	2.4977	9.616
S27	1800	190.48	1.3624	5.245
S28	1850	206.35	1.4759	5.682

S29	1900	158.73	1.1353	4.371
S30	1920	126.98	0.9082	3.497
S31	1950	126.98	0.9082	3.497
S32	2000	206.35	1.4759	5.682
S33	2050	174.6	1.2488	4.808
S34	2100	174.6	1.2488	4.808
S35	2150	95.238	0.6812	2.622
S36	2185	222.22	1.5894	6.119
S37	2200	190.48	1.3624	5.245
S38	2220	158.73	1.1353	4.371
S39	2250	190.48	1.3624	5.245
S40	2300	190.48	1.3624	5.245
S41	2350	126.98	0.9082	3.497
S42	2400	142.86	1.0218	3.934
S43	2450	238.1	1.7029	6.556
S44	2472	317.46	2.2706	8.742
S45	2500	238.1	1.7029	6.556
S46	2550	285.71	2.0435	7.868
S47	2600	238.1	1.7029	6.556
S48	2650	111.11	0.7947	3.0596
S49	2700	190.48	1.3624	5.245
S50	2750	142.86	1.0218	3.934
S51	2800	206.35	1.4759	5.682
S52	2850	142.86	1.0218	3.934
S53	2880	301.59	2.1571	8.305
S54	2900	126.98	0.9082	3.498
S55	2925	206.35	1.4759	5.682
S56	2950	126.98	0.9082	3.497
S57	3000	111.11	0.7947	3.0596
S58	3050	206.35	1.4759	5.682
S59	3295	111.11	0.7947	3.0596
S60	3520	190.48	1.3624	5.245
Average	-	170.511	1.23	4.76

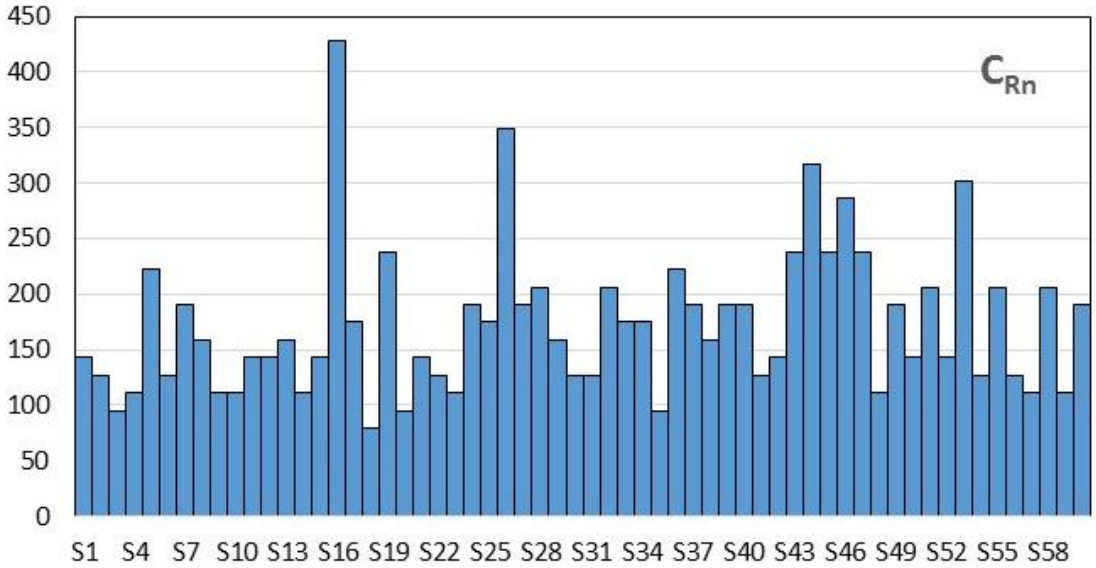

Figure 6. The radon concentration as a function of soil sample number.

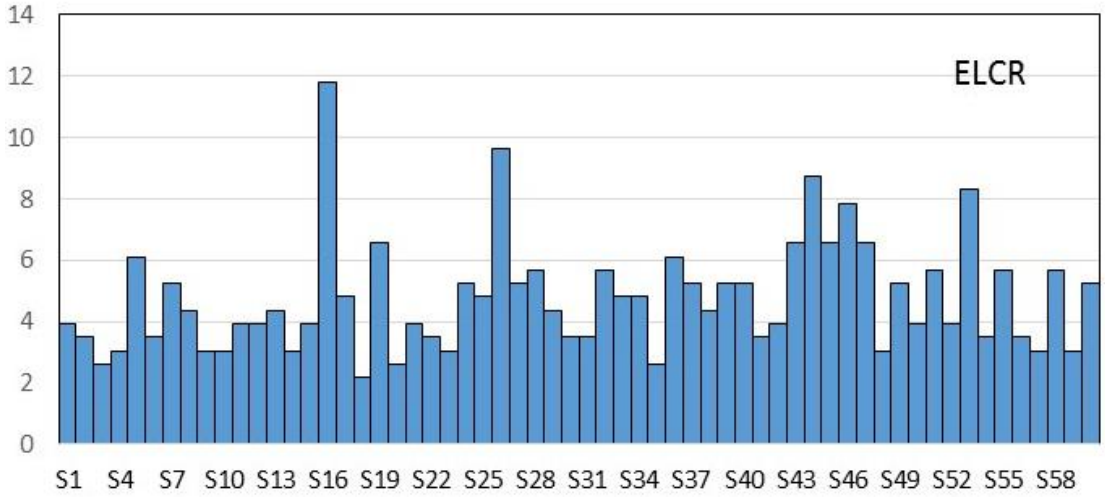

Figure 7. The ELCR as a function of soil samples number.

Conclusions

Radon represents a significant public health concern when present in indoor air. Epidemiological studies have consistently established a link between radon exposure in homes and an elevated risk of lung cancer within the general population. In the spectrum of lung cancer carcinogens, radon stands as the second most prominent contributor, following smoking. The radium concentrations ranged between (428.75 – 79.36) Becquerel / m^3, and the highest recommended limit ICRP (50-150) Bq / $\boldsymbol{m^3}$. It means the doses are higher than the limits allowed which indicates that workers in the oil fields and the neighboring population of these areas are exposed by high radon gas and elevated risk factor for lung cancer caused by radon. These findings suggest the necessity of formulating and implementing effective measures to prevent and mitigate indoor radon concentrations. Incorporating such measures into national radon control programs is crucial for safeguarding public health.

Conflicts of Interest: The authors declare no conflict of interest.

Funding Statement: No funding was received for this research.

References

[1] Abood, R. A; Abdahmed, K. A.; Sultan, S. S.; "Epidemiology of Different Types of Cancers Reported in Basra, Iraq". Qaboos Univ. Med J., 20 (3): 295–300, 2020.

[2] ICRP, Recommendations of the International Commission on Radiological Protection, Publication 60, 1990

[3] Iraq Body Count Project, "Gaps in recording and reporting suggest that even our highest totals to date may be missing many civilian deaths from violence." Iraq Body Count Project, 2017.

[4] Merrious, O.O.; Fredrick, O. U.; Ochuko, A., "Evaluation of natural radioactivity levels and radiation hazards of Nkalagu limestone deposit, southeastern Nigeria". Environmental Monitoring and Assessment, 196(12): 1176, 2024.

[5] Asia, H. Al-Mashhadani; Ali, H.S.; Yas, R.M.; Ali, K.S.; "Radon concentration measurement in a groundwater in Al-Tuz, Salah Al-Din Governorate using nuclear track detector CN-85". IOP Conference Series: Materials Science and Engineering, 757(1): 012015, 2020.

[6] James, E. T.; "Atoms, Radiation, and Radiation Protection". Third edition, Completely Revised and Enlarged Edition, 2007.

[7] Mohammed Salih L.M.; "Measurement of Radon Concentrations and Annual Dose Rate in some Regions of Baghdad City using LR-115 Nuclear Track Detector". J. Al-Nahrain Univ. Sci. 17(3): 94-98, 2014.

[8] Fischer B.E.; Sphor R., "Production and use of nuclear tracks: imprinting structure on solids" Rev. Mod. Phys. 55: 129, 1983.

[9] Onoja, R. A.; "Total radioactivity count in taps and well water around Zaria area, Kaduna State, Nigeria". Ph.D. thesis, ABU, Zaria. Nigeria , 2010.

[10] Kobayashi, T.; Fujii, M.; "Effect of various etching solutions on the response of CR-39", Nucl. Tracks, 15: 175, (1988).

[11] Tawfiq, N.F.; "Study Comparssion in Some of Organic and Inorganic Track Detectors and Applications in Environment". Ph.D thesis, University of Al-Mustansiriyah, (1996).

[12] Razzaq, D.F.; Saleh, D.S.; Asia, H. Al-Mashhadani, "Studying the uranium pollution in reduction the levels of the C-Peptide and Vitamin D for healthy and diabetic patients in Najaf City Iraq". AIP Conference Proceedings 2290: 0027502, 2020.

[13] Ali, Kh. Sh.; "Study of Radioactive Pollution in Oil Wells Waste and the Methods of Treatment, Master Thesis, University of Baghdad, 2021.

[14] Asia, H. Al-Mashhadani; Hassan, Z.,M.; "Radioactive wastewater treatment using magnetic nanocomposite material". International Journal of Drug Delivery Technology, 11(1): 244–247, 2021.

[15] Nichulas, T.; "Measurement and Detection of Radiation", Pergammon Press, University of Missouri-Rolla, U.K. 1987.
[16] Fremlin, J.H.; Wilson, C.R., "Nuclear track detection: advances and potential in astrophysics, particle physics and applied research". Nucl. Instr. Meth., 173: 201, 1980.
[17] Idan, R.; "Depositional Environments, Facies Distribution, and Porosity Analysis of Yamama Formation in Majnoon Oilfield. Sequence Stratigraphic Approach" Iraqi Geo. J. 53(1D): 38-52, 2020.
[18] UNSCEAR. Report, United Nations Scientific Committee on the Effects of Atomic Radiation Sources, sources and Effects of ionizing radiation, New York: United Nations Publication, 1986.
[19] Idan, R. M; Faisal, R. F.; "Application of Geophysical Logs to Estimate the Source Rock Quantity of Ratawi Formation, Southern Iraq: A Comparison Study". IOP Conf. Ser.: Mater. Sci. Eng. 579:012025, 2019.
[20] Ali, Kh. Sh.; Asia H. Al-Mashhadani; Abood W. K., "Assessment of lung cancer risk due to exposure to radon from oil well in (Majnoon) Basra". AIP Conference Proceedings, 2591: 030065, 2023.